Molecules and Cells

Recovery of TRIM25-Mediated RIG-I Ubiquitination through Suppression of NS1 by RNA Aptamers

Hye-Min Woo[1,2,5], Jin-Moo Lee[1,3,5], Chul-Joong Kim[4], Jong-Soo Lee[4], and Yong-Joo Jeong[1,*]

[1]School of Applied Chemistry, Kookmin University, Seoul 02707, Korea, [2]Division of Emerging Infectious Disease and Vector Research, Korea National Institute of Health, Cheongju 28159, Korea, [3]Pharmacological Research Division, National Institute of Food and Drug Safety Evaluation, Cheongju 28159, Korea, [4]College of Veterinary Medicine, Chungnam National University, Daejeon 34134, Korea, [5]These authors contributed equally to this work.
*Correspondence: jeongyj@kookmin.ac.kr
https://doi.org/10.14348/molcells.2019.0157
www.molcells.org

Non-structural protein 1 (NS1) of influenza virus has been shown to inhibit the innate immune response by blocking the induction of interferon (IFN). In this study, we isolated two single-stranded RNA aptamers specific to NS1 with K_d values of 1.62 ± 0.30 nM and 1.97 ± 0.27 nM, respectively, using a systematic evolution of ligand by exponential enrichment (SELEX) procedure. The selected aptamers were able to inhibit the interaction of NS1 with tripartite motif-containing protein 25 (TRIM25), and suppression of NS1 enabled retinoic acid inducible gene I (RIG-I) to be ubiquitinated regularly by TRIM25. Additional luciferase reporter assay and quantitative real-time PCR (RT-PCR) experiments demonstrated that suppression of NS1 by the selected aptamers induced IFN production. It is noted that viral replication was also inhibited through IFN induction in the presence of the selected aptamers. These results suggest that the isolated aptamers are strongly expected to be new therapeutic agents against influenza infection.

Keywords: aptamer, influenza virus, non-structural 1, systematic evolution of ligands by exponential enrichment, ubiquitination

INTRODUCTION

Influenza is a serious health threat causing occasional pandemics and seasonal epidemics. The causative agents, influenza viruses, belong to the family of *Orthomyxoviridae* and have single-stranded negative-sense RNA genome of 8 segments. Thus far, influenza is classified on the subtypes of 18 hemagglutinins and 11 neuraminidases (Tong et al., 2013).

To prevent the amplification of influenza, the host cells initiate innate immune response by recognizing conserved motif or pathogen-associated molecule patterns of incoming pathogen. This innate immunity is accomplished by pattern-recognition receptors such as the toll-like receptors (TLRs) (Kaisho and Akira, 2006) or retinoic acid inducible gene I (RIG-I)-like receptors (RLRs) of the host cells (Yoneyama and Fujita, 2004), followed by production of antiviral cytokine interferons (IFNs). To evade host's innate immune response, influenza has evolved a few strategies for viral replication. Influenza NS1 is known to be one of the most important proteins to counteract the antiviral IFN production of the host.

NS1 is encoded by segment 8 of the influenza and range in size 217-237 amino acids. NS1 is comprised of two functional domains, N-terminal RNA-binding domain (RBD) and C- terminal effector domain (ED). RBD, amino acids 1-73 of NS1, forms a six-helical homodimer, and its major role is

Received 13 July, 2019; revised 28 August, 2019; accepted 1 September, 2019; published online 10 October, 2019

eISSN: 0219-1032
©The Korean Society for Molecular and Cellular Biology. All rights reserved.
This is an open-access article distributed under the terms of the Creative Commons Attribution-NonCommercial-ShareAlike 3.0 Unported License. To view a copy of this license, visit http://creativecommons.org/licenses/by-nc-sa/3.0/.

double-stranded RNA (dsRNA) binding, thereby blocking IFN induction on infection (Pichlmair et al., 2006). ED also dimerizes and binds several cellular proteins (Aramini et al., 2011; Hale et al., 2008), which is responsible for sequence variations of different virus strains. In fact, NS1 has multiple functions in infected cells. Of the various functions, the major role of NS1 is the disruption of host cell innate immune system, and inhibits the induction of IFN (Garcia-Sastre et al., 1998; Kochs et al., 2007). Thus far, there have been many attempts to elucidate the molecular mechanism by which NS1 suppresses the IFN production. One explanation of the NS1 function is sequestration of viral RNA, which leads to inhibition of main viral RNA sensor RIG-I in the host cell (Chien et al., 2004). Strain-specific direct interaction between NS1 and RIG-I was also suggested. Jureka et al. (2015) demonstrated that RBD of 1918 H1N1 NS1 interacted directly with second caspase activation and recruitment domain (CARD) of RIG-I, but no interaction was observed in case of Udorn H3N2 strain. In addition to direct interaction, NS1 has been shown to inhibit tripartite motif-containing protein 25 (TRIM25)-mediated RIG-I ubiquitination, which suppresses the RIG-I signaling pathway (Gack et al., 2009). Regarding the RIG-I ubiquitination, two kinds of mechanism were suggested. After recognition of viral RNA harboring 5′-triphosphate by RIG-I, CARD is activated by either TRIM25-mediated ubiquitination (Gack et al., 2008) or binding of polyubiquitin chains that are previously synthesized by TRIM25 (Zeng et al., 2010). However, it is not clear how NS1 antagonizes IFN induction exactly at present. Because of the important role of NS1 during viral infection, many attempts have been made to develop antiviral therapeutics targeting NS1. This involves antiviral compounds (Engel, 2013), antisense oligonucleotides (Wu et al., 2014), nucleic acid aptamers (Woo et al., 2013), and so on.

In the present study, we isolated RNA aptamers specific to influenza NS1 protein. Because nucleic acid aptamers have comparable binding affinities with corresponding antibodies, they are regarded as potential candidates for the development of therapeutic agents or diagnostic probes (Brody and Gold, 2000). The selected RNA aptamers bind to NS1 specifically and inhibit the interaction between NS1 and TRIM25. This leads to recover TRIM25-mediated RIG-I ubiquitination and subsequent IFN induction. We also found that viral replication was suppressed in the presence of aptamers, which suggests that the selected RNA aptamers can be developed as a useful therapeutic agent in future.

MATERIALS AND METHODS

Cell culture

HEK293T (human embryonic kidney epithelial cell line) and Raw264.7 (murine macrophage cell line) cell lines were cultured in Dulbecco's modified minimal essential medium (DMEM) supplemented with 100 U penicillin-streptomycin and 10% fetal bovine serum at 37°C in a humidified atmosphere containing 5% CO_2.

Systematic evolution of ligands by exponential enrichment (SELEX) procedure

The RNA library was generated by *in vitro* transcription using 109 bp DNA library containing two primer regions and 40 random nucleotides as described previously (Jang et al., 2008). Recombinant GST-tagged NS1 was expressed in *Escherichia coli* and purified as described previously (Woo et al., 2013). For *in vitro* selection, 5 μg of the RNA library was incubated with 100 μl Glutathione-Sepharose 4B (GE Healthcare, USA) in 100 μl binding buffer (50 mM Tris/Cl [pH 8.0], 150 mM NaCl, 1.5 mM $MgCl_2$, 2 mM dithiothreitol [DTT] and 1% [w/v] bovine serum albumin [BSA]). The nonspecific RNAs bound to bead were precipitated and discarded. Unbound RNAs were reacted with the 2 μg GST-NS1 for 30 min at room temperature and then incubated with 100 μl Glutathione-Sepharose 4B for 30 min. NS1 complexed with RNA was dissociated from the Glutathione-Sepharose 4B by elution buffer (binding buffer + 10 mM glutathione). RNAs bound to NS1 was recovered by phenol-chloroform extraction and purified by ethanol precipitation. cDNA was synthesized from recovered RNAs by reverse-transcription and amplified by polymerase chain reaction (PCR). Total 15 rounds of selection were performed and the resulting DNA was cloned into the pGEM-T Easy vector (Promega, USA). After transformation into *E. coli*, plasmid DNA was obtained from individual clones and sequenced. The secondary structures of selected RNA aptamers were predicted using the Mfold program as described previously (Jang et al., 2008; Woo et al., 2013).

Measurement of the NS1 protein - RNA aptamer interaction by enzyme-linked immunosorbent assay (ELISA)

Glutathione coated plate (Pierce Biotechnology, USA) was incubated with 100 μl/well of GST-NS1 (100 nM in phosphate-buffered saline [PBS]) for 1 h at room temperature. The wells were blocked with 5% BSA in PBS with Tween 20 (PBST) for 1 h, and followed by incubation with various concentrations of aptamers (100 μl/well in PBS) for another 1 h at room temperature. Unbound GST-NS1 proteins were detected by incubating with 100 μl/well of NS1 antibody (1:1,000 in PBS; Santa Cruz Biotechnology, USA) and 100 μl/well of goat-anti-mouse-horseradish peroxidase (HRP) (1:1,000 in PBS; Santa Cruz Biotechnology) for 1 h at room temperature. After washing, 100 μl/well of 3,3′,5,5′-tetramethylbenzidine (TMB) solution (Merck, Germany) was added to detect the bound HRP. The color developing reaction was stopped with 0.5 N H_2SO_4 and the absorbance of each well was measured at 450 nm using a TRIAD microplate reader (Dynex Technologies, USA). The percentage of inhibition (Y axis) was calculated from the following equation: inhibition percentage = 100 − [(Abs/A_0) × 100], where Abs is the absorbance in the presence of aptamer and A_0 is the absorbance in the absence of aptamer.

Pull down assay

MBP-TRIM25 was prepared as described in Supplementary Materials. MBP-TRIM25 (10 μg) was immobilized on 10 μl of amylose beads for 1 h at room temperature. GST-NS1 (10 μg) was mixed with the 2 or 5 μg of selected aptamer for 1 h at room temperature, and then TRIM25 coated amylose beads were incubated with aptamer-NS1 complex for 1 h at room temperature. After four washes with PBS, the proteins bound to the beads were heated to 95°C for 2 min and ana-

lyzed by western blotting. MBP-TRIM25 and GST-NS1 were detected with MBP antibody-HRP (1:1,000 in PBST) and GST antibody-HRP (1:1,000 in PBST), respectively. The bands were visualized using an enhanced chemiluminescence (ECL) system and ImageQuant LAS4000 (GE Healthcare Bio-Sciences, USA).

In vitro ubiquitination assay

Ubiquitination assay was performed as described previously (Gack et al., 2007), with slight modifications. His-RIG-I was prepared as described in Supplementary Materials. The 2 μg His-RIG-I, 2 μg polyI:C, 2 μg MBP-TRIM25, 2 μg GST-NS1 and 2 μg aptamer in 50 μl of reaction buffer (50 mM Tris/Cl [pH 7.5], 2 mM dithiothreitol, 5 mM $MgCl_2$, and 4 mM ATP) were mixed with 5 μg ubiquitin (Boston Biochem, USA), 0.16 μg human recombinant E1 (Sigma-Aldrich, USA), and 2 μg human recombinant UbcH5a (Pierce Biotechnology). The reaction mixture was incubated for 2 h at 32°C, and subjected to immunoblotting with anti-RIG-I antibody, anti-ubiquitin antibody, anti-MBP antibody, and anti-GST antibody, respectively.

Luciferase reporter gene assay

For a luciferase reporter gene assay, 1 × 10^6 HEK293T cells were plated in a tissue culture dish (10 cm diameter) and then incubated for 24 h, after which they were transfected with 7.5 μg of p4xκB and 2.5 μg of pGL using Fugene HD (Roche, Germany) as described previously (Woo et al., 2013) with slight modification. After 24 h incubation, cells were detached, plated in a 24-well plate (5 × 10^4), and then further incubated for 24 h. Subsequently, cells were transfected with 0.5 μg of pcDNA6-AIV NS1 and the indicated amount of aptamers using lipofectamine™ 2000 (Thermo Fisher Scientific, USA). After 6 h incubation, NF-κB was induced by substituting the medium with DMEM containing 1% polyI:C. After 48 h, cells were lysed and the cell lysates were used to measure luciferase activities by Dual-luciferase Reporter Assay system (Promega). The luminescences of firefly luciferase and Renilla luciferase were measured using VICTOR X3 multilabel plate reader (PerkinElmer, USA), and the firefly luciferase activity was normalized to that of Renilla luciferase.

Quantification of IFN-β by RT-PCR

HEK293T cells (5 × 10^4) were transfected with 0.5 μg of pcDNA6-AIV NS1 and the indicated amount of aptamers using lipofectamine™ 2000. After 6 h incubation, the media was substituted with DMEM containing 1% polyI:C. After 48 h, total RNA was isolated using easy-BLUE™ Total RNA Extraction kit (iNtRON Biotechnology, Korea), according to the manufacturer's instructions. The concentration of RNA was determined by measurement of the absorbance at 260 nm. Extracted RNA (1 μg) was used to synthesize cDNA using Maxim RT premix kit (iNtRON Biotechnology), according to the manufacturer's instructions. Quantitative real-time PCR (qPCR) was performed using synthesized cDNA and the SYBR green PCR Master Mix by a StepOnePlus™ (Applied Biosystems, USA). The PCR consists of a 10 min polymerase enzyme activation step at 95°C, and 40 cycles of denaturation at 95°C for 15 s, and annealing/extension at 60°C for 1 min. The following primer pairs were used: INF-β forward prim-

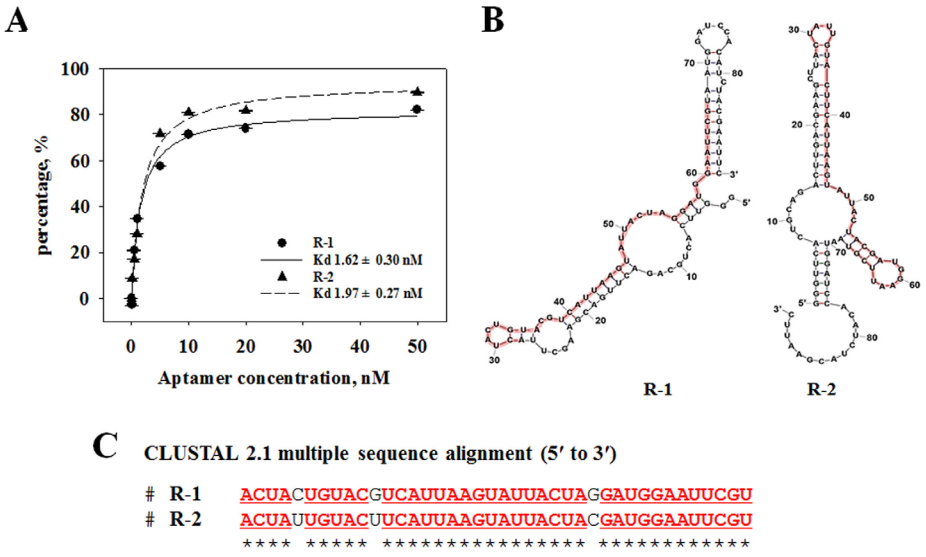

Fig. 1. Isolation of RNA aptamers specific to NS1 protein. (A) Measurement of the affinities of the selected aptamers. The immobilized GST-tagged NS1 proteins were incubated with increasing concentrations of the selected RNA aptamers (R-1 and R-2). After addition of primary and secondary antibodies sequentially, inhibition percentage was calculated. The graphs were fit to the Michaelis-Menten equation and the values of the K_d were calculated (1.62 ± 0.30 nM [R-1] and 1.92 ± 0.27 nM [R-2]). (B) The predicted secondary structure of R-1 and R-2 using Zuker's Mfold program. Shaded nucleotides indicate the central 40 random sequences of the selected aptamers. (C) Comparison of the central 40 random sequences of the selected aptamers. Conserved sequences identified by ClustalW2 were indicated by asterisks and underlines.

er (5′-AAACTCATGAGCAGTCTGCA-3′), INF-β reverse primer (5′-AGGAGATCTTCAGTTTCGGAGG-3′); human β-actin forward primer (5′-AGCGAGCATCCCCCAAAGTT-3′), human β-actin reverse primer (5′-AGGGCACGAAGGCTCATCATT-3′). The relative quantification was performed according to the delta-delta *C*t model (Livak and Schmittgen, 2001): amount of target = $2^{-[\Delta C\,t\,INF\text{-}\beta - \Delta C\,t\,\beta\text{-actin}]}$, where *C*t is the threshold cycle).

Inhibition of viral replication by NS1 aptamer on RAW 264.7 cells

To measure the viral replication inhibition by NS1 aptamer, various amounts of aptamers (0, 100, 200, 400, 600, 800, and 1,000 ng in 1 ml culture media) were added to Raw264.7 cells and incubated for 6 h prior to infection of influenza virus containing PR8–green fluorescent protein (GFP) as described previously (Woo et al., 2013). After 12 h, the GFP expression was observed using fluorescence microscope and the measured GFP relative units were fit to a hyperbolic decay equation.

Statistical analysis

Group comparisons were performed by a paired Student's *t*-test in Prism 7 (GraphPad Software, USA). Differences were considered significant when *P* values were less than 0.05.

RESULTS

Selection of RNA aptamers specific to NS1 protein

To isolate high-affinity RNA aptamers for NS1 protein, we performed SELEX procedure using a RNA library pool containing central 40 random core sequences. After 15 rounds of selection, 9 independent RNA aptamers were isolated and sequenced (data not shown). The binding affinity of each aptamer for NS1 protein was determined by ELISA with NS1 antibody and expressed as K_d values. The NS1 proteins were immobilized on glutathione-coated plates and various concentrations of the 9 selected RNA aptamers were added. And then NS1 antibody and anti-mouse-HRP were added. After addition of TMB, the reaction was stopped and the absorbance was measured at 450 nm. After calculation of inhibition percentage, the curve was fit to a Michaelis–Menten equation (inhibition percentage = A[NS1] / (K_d + [NS1], where A is the amplitude, [NS1] is the concentration of NS1, and K_d is the dissociation constant), and the amplitude and K_d value of each RNA aptamer were obtained (data not shown). Of the 9 aptamer candidates, two aptamers named R-1 (K_d = 1.62 ± 0.30 nM) and R-2 (K_d = 1.92 ± 0.27 nM) were found to have the highest binding affinities for NS1 (Fig. 1A). From the results of ELISA, we also found that the selected aptamers were able to interfere with NS1-NS1 antibody interaction. Based on the determination of binding affinity, the selected RNA aptamers were further analyzed bioinformatically. The secondary structures of the isolated RNA aptamers were predicted by Mfold program (Zuker, 2003) and shown in Figure 1B. The central 40 nucleotide random sequence region of the selected RNA aptamer was indicated by shaded line. Further bioinformatic analysis was performed by ClustalW2 (Cheng et al., 2008) as shown in Figure 1C. ClustalW2 was used to compare the nucleic acid sequence similarity of R-1 and R-2, and the result showed that they have 90% sequence identity.

Inhibition of NS1-TRIM25 interaction by the selected aptamers

In order to ensure that the selected aptamers can inhibit the interaction between TRIM25 and NS1, the pull-down assays

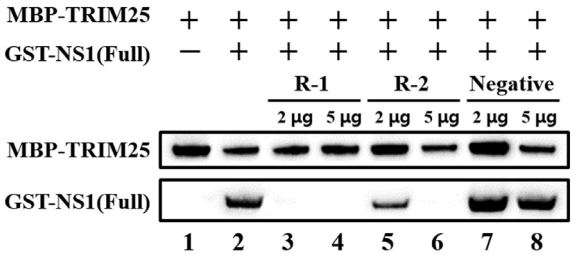

Fig. 2. Inhibition of NS1-TRIM25 interaction by the selected aptamers. MBP-TRIM25 was immobilized on amylose beads and GST-NS1 was pre-mixed with the selected aptamers (R-1 and R-2). TRIM25 coated amylose beads were incubated with aptamer-NS1 complex, washed, and analyzed by western blotting to investigate the interaction of TRIM25 with NS1. Lane 1, without NS1 and aptamers in the presence of TRIM25; Lane 2, without aptamers in the presence of TRIM25 and NS1; Lane 3, included 2 μg of R-1 aptamer in the presence of TRIM25 and NS1; Lane 4, included 5 μg of R-1 aptamer in the presence of TRIM25 and NS1; Lane 5, included 2 μg of R-2 aptamer in the presence of TRIM25 and NS1; Lane 6, included 5 μg of R-2 aptamer in the presence of TRIM25 and NS1; Lane 7, included 2 μg of RNA library in the presence of TRIM25 and NS1 as a negative control; Lane 8, included 5 μg of RNA library in the presence of TRIM25 and NS1 as a negative control.

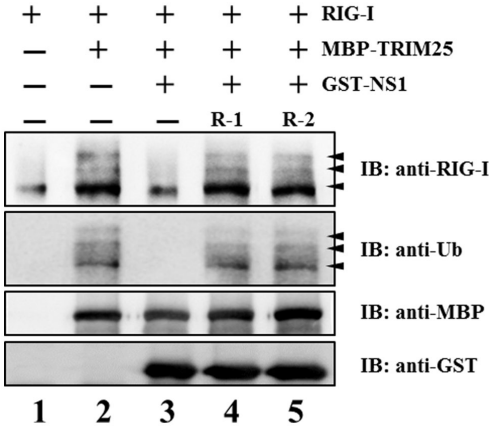

Fig. 3. Recovery of TRIM25-mediated RIG-I ubiquitination by aptamers specific to NS1. *In vitro* ubiquitination was detected by immunoblotting as described in Materials and Methods. In the presence of R-1 and R-2 aptamers, regular ubiquitination was occurred by suppressing the NS1 activity (lanes 4 and 5). Arrows indicate ubiquitinated bands.

were performed. The MBP-TRIM25 coated amylose beads were incubated with NS1 in the absence or presence of aptamers, and analyzed by western blot (Fig. 2). Lane 2 shows that TRIM25 interacts with NS1 in the absence of aptamer. However, the interaction between TRIM25 and NS1 was suppressed in the presence of aptamers (lanes 3-6). Whereas we were not able to detect any band intensity in the presence of 2 μg R-1 aptamer (lane 3), band intensities decreased as the amount of R-2 aptamer increased (lanes 5 and 6). RNA library was used instead of aptamer as a negative control (lanes 7 and 8). It indicates that the selected aptamers inhibit the interaction of TRIM25 with NS1 in a dose-dependent manner.

Recovery of TRIM25 mediated RIG-I ubiquitination through inhibition of NS1 by the selected aptamers

We hypothesized that TRIM25 can ubiquitinate the RIG-I regularly if NS1 is not working properly through inhibition by the selected aptamers. To test this hypothesis, we investigated whether the selected aptamers inhibit the function of the NS1 and lead to regular TRIM25-mediated RIG-I ubiquitination by carrying out the *in vitro* ubiquitination assay (Fig. 3). When RIG-I was incubated with TRIM25, RIG-I was ubiquitinated and not ubiquitinated in the absence (lane 2) and presence of NS1 (lane 3), respectively, which is consistent with previous report (Gack et al., 2007; 2009). However, if we included the selected aptamers in the reaction mixtures, RIG-I was able to interact with TRIM25 and ubiquitinated without being interfered by NS1 (lanes 4 and 5). These results indicate that the selected aptamers suppress the NS1 activity and TRIM25-mediated RIG-I ubiquitination occurs regularly.

Induction of IFN by the selected RNA aptamers

Because TRIM25 mediated RIG-I ubiquitination was observed by suppressing the NS1, we performed cell based NF-κB luciferase reporter assay to determine whether the selected aptamers promote the induction of IFN. Figure 4A shows that NF-κB transcriptional activity was increased as the amount of the aptamers increased. HEK293T cells transfected with an NS1 vector (MOCK) showed about 60% decrease of luciferase activity compared to positive control (Naïve). However, dose-dependent increase of luciferase activity was observed after addition of the selected aptamers. Additional quantitative RT-PCR experiment showed that the induction of IFN was recovered by the selected aptamers. After HEK293T cells were transfected with an NS1 vector, various amounts of the selected aptamers were added and the total RNA was extracted. Then, qPCR was performed to quantify the cDNA using IFN-β and β-actin-specific primers. The result showed that mRNA expression level increased as the amount of the selected aptamers increased (Fig. 4B), similar to the result of luciferase reporter assay. Taken together, our results demonstrate that the selected RNA aptamers binds to NS1, and recovery of RIG-I ubiquitination by TRIM25 induces IFN production.

Inhibition of influenza virus replication by the RNA aptamers

To determine whether the selected aptamers inhibit the viral replication, Raw264.7 cells harboring GFP were treated with the aptamers prior to viral infection, followed by measurement of fluorescence. Figure 5 shows that the selected aptamers can suppress the viral replication dramatically even in the presence of 100 ng of aptamers (approximately less than half of fluorescence unit compared to 0 ng treated). When we added 200 ng of aptamers, the fluorescence level already reached to level of a positive control (IFN-β). The GFP relative unit decreased in a hyperbolic manner with increasing amount of aptamers providing a 50% inhibitory concentration of 48.20 ± 6.47 ng/ml (R-1, equivalent to 1.66 ± 0.22 nM) and 55.07 ± 4.36 ng/ml (R-2, equivalent to 1.90 ± 0.15 nM), respectively. However, we were not able to detect any

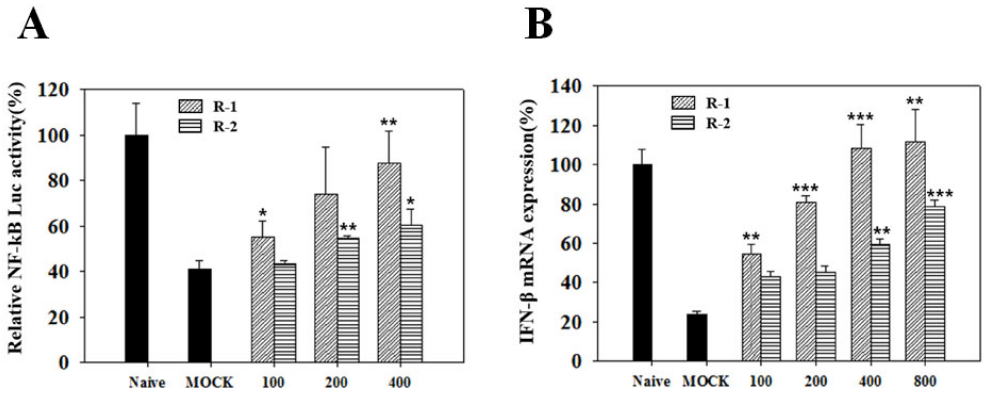

Fig. 4. IFN-β induction by inhibition of NS1. (A) HEK293T cells were cotransfected with plasmids encoding the NF-κB luciferase reporter construct, Renilla luciferase, NS1, and increasing amounts (0, 100, 200, and 400 ng) of aptamers. The value was calculated as the ratio between the NF-κB luciferase and the Renilla luciferase, corrected by naive and represented as a ratio at the y-axis. (B) HEK293T cells were transfected with NS1 and increasing amounts (0, 100, 200, 400, and 800 ng) of aptamers. Total mRNA was isolated, and the production of IFN-β mRNA was quantitated by real-time PCR. The measured *C*t value by real-time PCR was converted to the amount of IFN-β relative to β-actin by the delta-delta *C*t model equation, which is expressed on the y-axis as a ratio to the naïve. The data represents average values after 3 independent experiments. Naïve, HEK293T cells only; MOCK, cells transfected with only NS1. Data are expressed as mean ± SD. $*P \leq 0.05$, $**P \leq 0.005$, $***P \leq 0.0005$.

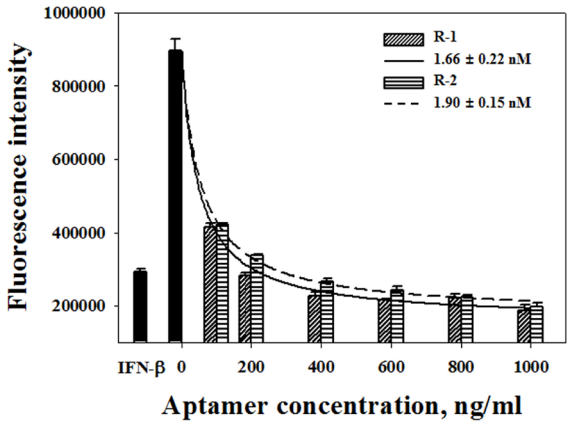

Fig. 5. Suppression of viral replication by the selected aptamers. Viral replication assay was performed with various amounts of aptamers (0, 100, 200, 400, 600, 800, and 1,000 ng). The transfected Raw264.7 cells were infected with PR8-GFP virus, and measured fluorescence signals that represented virus viability. The recombinant mouse IFN-β 1,000 units/ml was used as a positive control (lane INF-β). The fluorescence intensity versus (aptamers) fit to a hyperbolic decay equation, which provides 50% inhibitory concentration.

cytotoxicity regardless of the amount of aptamer used (data not shown).

DISCUSSION

To cope with invasion of incoming pathogens, host cells have a self-defense system, innate immune response, such as TLRs or RIG-I like receptors. One of the primary roles in innate immunity is induction of IFN, antiviral cytokine of the host cells. Most of viruses have evolved strategies to circumvent the host's innate immune response by inhibition of IFN production. Influenza also has such an IFN blocking system, NS1, which is able to antagonize IFN induction by preventing IRF-3 and NF-κB from activation. Therefore, NS1 is regarded as a good target for development of therapeutic agents such as small organic compounds and nucleic acids (Basu et al., 2009; Woo et al., 2013). Regarding the molecular mechanism how NS1 suppresses the IFN production, as of yet, precise mechanism remains unclear even though many attempts have been made. However, of the suggested mechanisms relevant to RIG-I pathway, it is most likely that NS1 interferes with RIG-I signaling pathway by inhibiting the RIG-I ubiquitination by E3 ligase TRIM25 (Gack et al., 2008; Zeng et al., 2010).

In this study, we isolated two RNA aptamers that specifically bind to and inhibit the function of NS1. One hundred nine bases ssRNA pool containing 40 random sequences in the central region was constructed by *in vitro* transcription using DNA library. When we analyzed binding affinities of the selected aptamers, about 1 nM K_d values were obtained. In addition, both aptamers showed 90% sequence identity each other. In fact, we performed similar experiments to select the ssDNA aptamers specific to NS1 and reported previously (Woo et al., 2013). When we compared the binding affinities of RNA aptamers with DNA aptamer (18.91 ± 3.95 nM in case of ssDNA aptamer), RNA aptamers showed almost ten times higher K_d value, indicating that RNA aptamer is better binding agent than DNA aptamer. This is consistent with the fact that RNA can accommodate more variable structures than DNA. When the two selected RNA aptamers were analyzed structurally using Mfold, the central 40 random sequences were shown to form a stem-loop-stem with a small hairpin. Because three-dimensional information is not available at present, further investigation will be necessary to determine exactly how the stem-loop-stem structure plays a role in NS1 binding. Determination of the binding region of the selected RNA aptamers to NS1 showed similar binding pattern with the case of ssDNA aptamer (Supplementary Fig. S1), which was published previously (Woo et al., 2013). RBD, not ED, of NS1 is the region to which the selected RNA aptamers were bound, and R38 amino acid is necessary for RNA aptamer binding. The reason why ssRNA and ssDNA aptamers showed similar binding to NS1 is not clear at present. According to the prediction of secondary structure by Mfold, the two kinds of nucleic acid aptamers do not show structural resemblance, although both of them inhibit the function of NS1. Thus far, crystal structure of each domain of NS1, RBD and ED, has been determined (Bornholdt and Prasad, 2006; Liu et al., 1997). However, considering the three-dimensional structure of full-length wild type NS1 is not available as of yet, further investigation will be necessary to understand the protein structure-aptamer binding relationship.

We carried out pull down assay to determine whether the selected RNA aptamers can inhibit the direct interaction between NS1 and TRIM25. NS1 is a multifunctional protein and known to interact with more than 50 proteins (Marc, 2014). Of many protein partners of the NS1, TRIM25 is involved in RIG-I signaling pathway, and sequestration of TRIM25 by NS1 leads to block the activation of RIG-I CARD. Although interaction mode is not clear in the present study, the selected aptamers were able to successfully inhibit the interaction of NS1 with TRIM25. This implies that the aptamers is effective in protecting the TRIM25 from NS1, thereby promoting the induction of IFN. We further investigated the effect of the selected aptamers on the RIG-I ubiquitination, which is necessary for RIG-I CARD to bind to a downstream protein partner, MAVS, of mitochondria (Cui et al., 2008). It has been shown that NS1 blocks the RIG-I signaling pathway by inhibiting the TRIM25-mediated RIG-I CARD ubiquitination, which leads to suppression of IFN induction (Gack et al., 2009). Our results revealed that the selected aptamers specifically bind to and block the function of NS1, thereby recovering the regular function of TRIM25 and subsequent RIG-I ubiquitination (Fig. 3). Therefore, this is consistent with the result of previous report (Gack et al., 2009). After verification of successful introduction of the selected aptamers into HEK293T cells by confocal images (Supplementary Fig. S2) and FACS analysis (Supplementary Fig. S3), further investigations also showed that the selected aptamers can induce IFN (Fig. 4) and subsequent block the viral replication (Fig. 5). Our results indicate that a blocking the NS1 function is one of the most

promising strategies to inhibit the viral replication. In fact, in addition to nucleic acid aptamer, many attempts have been made to discover small molecule-based NS1 antagonists targeting the interaction of NS1-dsRNA or NS1-protein partners (Engel, 2013).

In the present study, we showed that the recovery of TRIM25-mediated RIG-I ubiquitination is sufficient to induce IFN. Although it is not certain that the selected aptamers can inhibit the interaction of NS1 with dsRNA or protein partners of the host other than TRIM25 at present, we think that the binding of aptamers may cause a conformational change of NS1 and destroy the binding ability with binding partners, which will be the topic of our future study. Here, we simply focused on NS1-TRIM25 interaction and RIG-I ubiquitination. By selection of ssRNA aptamers specific to NS1, TRIM25-mediated RIG-I ubiquitination was recovered, and subsequent IFN induction and inhibition of viral replication were observed. Therefore, based on our results, we expect that more elaborated aptamer-based therapeutic agent will be developed through further studies.

Note: Supplementary information is available on the Molecules and Cells website (www.molcells.org).

Disclosure

The authors have no potential conflicts of interest to disclose.

ACKNOWLEDGMENTS

This work was supported by a grant of the Korea Health Technology R&D Project through the Korea Health Industry Development Institute (KHIDI), funded by the Ministry of Health & Welfare, Republic of Korea (grant No. HI15C2917).

ORCID

Hye-Min Woo https://orcid.org/0000-0001-8020-3489
Jin-Moo Lee https://orcid.org/0000-0001-5895-0277
Chul-Joong Kim https://orcid.org/0000-0001-8827-6332
Jong-Soo Lee https://orcid.org/0000-0001-5119-0711
Yong-Joo Jeong https://orcid.org/0000-0002-4735-0556

REFERENCES

Aramini, J.M., Ma, L.C., Zhou, L., Schauder, C.M., Hamilton, K., Amer, B.R., Mack, T.R., Lee, H.W., Ciccosanti, C.T., Zhao, L., et al. (2011). Dimer interface of the effector domain of non-structural protein 1 from influenza A virus: an interface with multiple functions. J. Biol. Chem. *286*, 26050-26060.

Basu, D., Walkiewicz, M.P., Frieman, M., Baric, R.S., Auble, D.T., and Engel, D.A. (2009). Novel influenza virus NS1 antagonists block replication and restore innate immune function. J. Virol. *83*, 1881-1891.

Bornholdt, Z.A. and Prasad, B.V. (2006). X-ray structure of influenza virus NS1 effector domain. Nat. Struct. Mol. Biol. *13*, 559-560.

Brody, E.N. and Gold, L. (2000). Aptamers as therapeutic and diagnostic agents. J. Biotechnol. *74*, 5-13.

Cheng, C., Dong, J., Yao, L., Chen, A., Jia, R., Huan, L., Guo, J., Shu, Y., and Zhang, Z. (2008). Potent inhibition of human influenza H5N1 virus by oligonucleotides derived by SELEX. Biochem. Biophys. Res. Commun. *366*, 670-674.

Chien, C.Y., Xu, Y., Xiao, R., Aramini, J.M., Sahasrabudhe, P.V., Krug, R.M., and Montelione, G.T. (2004). Biophysical characterization of the complex between double-stranded RNA and the N-terminal domain of the NS1 protein from influenza A virus: evidence for a novel RNA-binding mode. Biochemistry *43*, 1950-1962.

Cui, S., Eisenacher, K., Kirchhofer, A., Brzozka, K., Lammens, A., Lammens, K., Fujita, T., Conzelmann, K.K., Krug, A., and Hopfner, K.P. (2008). The C-terminal regulatory domain is the RNA 5'-triphosphate sensor of RIG-I. Mol. Cell *29*, 169-179.

Engel, D.A. (2013). The influenza virus NS1 protein as a therapeutic target. Antiviral Res. *99*, 409-416.

Gack, M.U., Albrecht, R.A., Urano, T., Inn, K.S., Huang, I.C., Carnero, E., Farzan, M., Inoue, S., Jung, J.U., and Garcia-Sastre, A. (2009). Influenza A virus NS1 targets the ubiquitin ligase TRIM25 to evade recognition by the host viral RNA sensor RIG-I. Cell Host Microbe *5*, 439-449.

Gack, M.U., Kirchhofer, A., Shin, Y.C., Inn, K.S., Liang, C., Cui, S., Myong, S., Ha, T., Hopfner, K.P., and Jung, J.U. (2008). Roles of RIG-I N-terminal tandem CARD and splice variant in TRIM25-mediated antiviral signal transduction. Proc. Natl. Acad. Sci. U. S. A. *105*, 16743-16748.

Gack, M.U., Shin, Y.C., Joo, C.H., Urano, T., Liang, C., Sun, L., Takeuchi, O., Akira, S., Chen, Z., Inoue, S., et al. (2007). TRIM25 RING-finger E3 ubiquitin ligase is essential for RIG-I-mediated antiviral activity. Nature *446*, 916-920.

Garcia-Sastre, A., Egorov, A., Matassov, D., Brandt, S., Levy, D.E., Durbin, J.E., Palese, P., and Muster, T. (1998). Influenza A virus lacking the NS1 gene replicates in interferon-deficient systems. Virology *252*, 324-330.

Hale, B.G., Barclay, W.S., Randall, R.E., and Russell, R.J. (2008). Structure of an avian influenza A virus NS1 protein effector domain. Virology *378*, 1-5.

Jang, K.J., Lee, N.R., Yeo, W.S., Jeong, Y.J., and Kim, D.E. (2008). Isolation of inhibitory RNA aptamers against severe acute respiratory syndrome (SARS) coronavirus NTPase/Helicase. Biochem. Biophys. Res. Commun. *366*, 738-744.

Jureka, A.S., Kleinpeter, A.B., Cornilescu, G., Cornilescu, C.C., and Petit, C.M. (2015). Structural Basis for a Novel Interaction between the NS1 Protein Derived from the 1918 Influenza Virus and RIG-I. Structure *23*, 2001-2010.

Kaisho, T. and Akira, S. (2006). Toll-like receptor function and signaling. J. Allergy Clin. Immunol. *117*, 979-987; quiz 988.

Kochs, G., Garcia-Sastre, A., and Martinez-Sobrido, L. (2007). Multiple anti-interferon actions of the influenza A virus NS1 protein. J. Virol. *81*, 7011-7021.

Liu, J., Lynch, P.A., Chien, C.Y., Montelione, G.T., Krug, R.M., and Berman, H.M. (1997). Crystal structure of the unique RNA-binding domain of the influenza virus NS1 protein. Nat. Struct. Biol. *4*, 896-899.

Livak, K.J. and Schmittgen, T.D. (2001). Analysis of relative gene expression data using real-time quantitative PCR and the $2^{-\Delta\Delta CT}$ method. Methods *25*, 402-408.

Marc, D. (2014). Influenza virus non-structural protein NS1: interferon antagonism and beyond. J. Gen. Virol. *95*, 2594-2611.

Pichlmair, A., Schulz, O., Tan, C.P., Naslund, T.I., Liljestrom, P., Weber, F., and Reis e Sousa, C. (2006). RIG-I-mediated antiviral responses to single-stranded RNA bearing 5'-phosphates. Science *314*, 997-1001.

Tong, S., Zhu, X., Li, Y., Shi, M., Zhang, J., Bourgeois, M., Yang, H., Chen, X., Recuenco, S., Gomez, J., et al. (2013). New world bats harbor diverse influenza A viruses. PLoS Pathog. *9*, e1003657.

Woo, H.M., Kim, K.S., Lee, J.M., Shim, H.S., Cho, S.J., Lee, W.K., Ko, H.W., Keum, Y.S., Kim, S.Y., Pathinayake, P., et al. (2013). Single-stranded DNA aptamer that specifically binds to the influenza virus NS1 protein suppresses interferon antagonism. Antiviral Res. *100*, 337-345.

Wu, N.C., Young, A.P., Al-Mawsawi, L.Q., Olson, C.A., Feng, J., Qi, H., Luan, H.H., Li, X., Wu, T.T., and Sun, R. (2014). High-throughput identification of loss-of-function mutations for anti-interferon activity in the influenza A virus NS segment. J. Virol. *88*, 10157-10164.

Yoneyama, M. and Fujita, T. (2004). [RIG-I: critical regulator for virus-induced innate immunity]. Tanpakushitsu Kakusan Koso *49*, 2571-2578.

Japanese.

Zeng, W., Sun, L., Jiang, X., Chen, X., Hou, F., Adhikari, A., Xu, M., and Chen, Z.J. (2010). Reconstitution of the RIG-I pathway reveals a signaling role of unanchored polyubiquitin chains in innate immunity. Cell *141*, 315-330.

Zuker, M. (2003). Mfold web server for nucleic acid folding and hybridization prediction. Nucleic Acids Res. *31*, 3406-3415.